

Journal Pre-proofs

1,3-Disubstituted Urea Derivatives: Synthesis, Antimicrobial Activity Evaluation and *In Silico* Studies

Miyase Gözde Gündüz, Sümeyye Buran Uğur, Funda Güney, Ceren Özkul, Vagolu Siva Krishna, Serdal Kaya, Dharmarajan Sriram, Şengül Dilem Doğan

PII: S0045-2068(20)31401-2
DOI: <https://doi.org/10.1016/j.bioorg.2020.104104>
Reference: YBIOO 104104

To appear in: *Bioorganic Chemistry*

Received Date: 28 April 2020
Revised Date: 29 June 2020
Accepted Date: 14 July 2020

Please cite this article as: M. Gözde Gündüz, S. Buran Uğur, F. Güney, C. Özkul, V. Siva Krishna, S. Kaya, D. Sriram, S. Dilem Doğan, 1,3-Disubstituted Urea Derivatives: Synthesis, Antimicrobial Activity Evaluation and *In Silico* Studies, *Bioorganic Chemistry* (2020), doi: <https://doi.org/10.1016/j.bioorg.2020.104104>

This is a PDF file of an article that has undergone enhancements after acceptance, such as the addition of a cover page and metadata, and formatting for readability, but it is not yet the definitive version of record. This version will undergo additional copyediting, typesetting and review before it is published in its final form, but we are providing this version to give early visibility of the article. Please note that, during the production process, errors may be discovered which could affect the content, and all legal disclaimers that apply to the journal pertain.

© 2020 Published by Elsevier Inc.



1,3-Disubstituted Urea Derivatives: Synthesis, Antimicrobial Activity Evaluation and *In Silico* Studies

Miyase Gözde Gündüz^a, Sümeyye Buran Uğur^b, Funda Güney^b, Ceren Özkul^c, Vagolu Siva Krishna^d, Serdal Kaya^{e,f}, Dharmarajan Sriram^d, Şengül Dilem Doğan^{b*}

^aDepartment of Pharmaceutical Chemistry, Faculty of Pharmacy, Hacettepe University, Sıhhiye, 06100 Ankara, Turkey

^bDepartment of Basic Sciences, Faculty of Pharmacy, Erciyes University, Kayseri, Turkey

^cDepartment of Pharmaceutical Microbiology, Faculty of Pharmacy, Hacettepe University, Sıhhiye, 06100 Ankara, Turkey

^dDepartment of Pharmacy, Birla Institute of Technology and Science-Pilani, Hyderabad, 500078, India

^eDepartment of Chemistry, Faculty of Arts and Sciences, Giresun University, 28200, Giresun, Turkey

^fDepartment of Aeronautical, Faculty of Aviation and Space Sciences, Necmettin Erbakan University, 42140, Konya, Turkey

*Corresponding author

Dr. Şengül Dilem Doğan

Address: Erciyes University
Faculty of Pharmacy
Department of Basic Sciences
38039
Kayseri, TURKEY

E-mail address: dogandilem@gmail.com

Phone number: +90 352 2076666-28032

Abstract

The development of new antimicrobial compounds is in high demand to overcome the emerging drug resistance against infectious microbial pathogens. In the present study, we carried out the extensive antimicrobial screening of disubstituted urea derivatives. In addition to the classical synthesis of urea compounds by the reaction of amines and isocyanates, we also applied a new route including bromination, oxidation and azidation reactions, respectively, to convert 2-amino-3-methylpyridine to 1,3-disubstituted urea derivatives using various amines. The evaluation of antimicrobial activities against various bacterial strains, *Candida albicans* as well as *Mycobacterium tuberculosis* resulted in new active agents. Among them, two compounds, which have the lowest MIC values on *Pseudomonas aeruginosa*, were further evaluated for their inhibition capacities of biofilm formation. In order to evaluate their potential mechanism of biofilm inhibition, these two compounds were docked into the active site of LasR, which is the transcriptional regulator of bacterial signaling mechanism known as quorum sensing. Finally, the theoretical parameters of the bioactive molecules were calculated to establish their drug-likeness properties.

Keywords: antibacterial, tuberculosis, antifungal, biofilm, molecular docking, quorum sensing

1. Introduction

Infectious diseases, caused by Gram-positive/Gram-negative, fungal and mycobacterial pathogens, still seriously jeopardize human health despite existing for centuries [1]. Together with cancer and cardiovascular diseases, bacterial infections stand among the leading causes of serious morbidity and mortality all over the world [2]. Amongst different microbial infections, the incidence of fungal infections has dramatically increased over the previous decades especially in immunocompromised patients with AIDS diagnose, organ transplant history or cancer chemotherapy process [3]. Tuberculosis, caused by *Mycobacterium tuberculosis*, is an infectious pulmonary disease and is the foremost reason for life lost owing to a single infectious agent. The World Health Organization approximated ten million patients developed TB in 2017 [4].

The primary obstruction to the achievement of a successful chemotherapy regimen in infectious diseases is the growing antimicrobial resistance to the present drugs [5]. Therefore, the discovery of new and more effective therapeutic agents with favorable pharmacokinetic profiles is of utmost importance.

Pseudomonas aeruginosa is a Gram-negative bacterium and is considered as one of the most opportunistic pathogens causing life-threatening infections in diseases such as meningitis, septicemia and cystic fibrosis [6]. It is also responsible for the considerable mortality in immunocompromised patients. Additionally, *P. aeruginosa* is capable of producing biofilm which reduces the effectiveness of therapeutic agents and increases the antibacterial resistance [7]. Biofilm formation is attributed to the communication of bacteria via the signaling mechanism called quorum sensing (QS). LasR is the transcriptional regulator of QS and plays a key role in the pathogenesis of *P. aeruginosa* [8]. *N*-Acyl homoserine lactones (AHLs) are a class of signaling molecules employed in bacterial QS (Figure 1) [9].

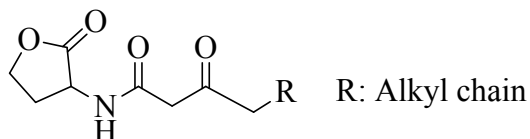


Figure 1. General chemical structure of AHLs

The chemical structures of AHLs differ according to the bacteria species. 3-oxo-dodecanoyl homoserine lactone (ODHL) is found in *P. aeruginosa* and is recognized by LasR with the defined interactions (Figure 2) [9]. Therefore, inhibiting this system is a rational approach to decrease bacterial virulence.

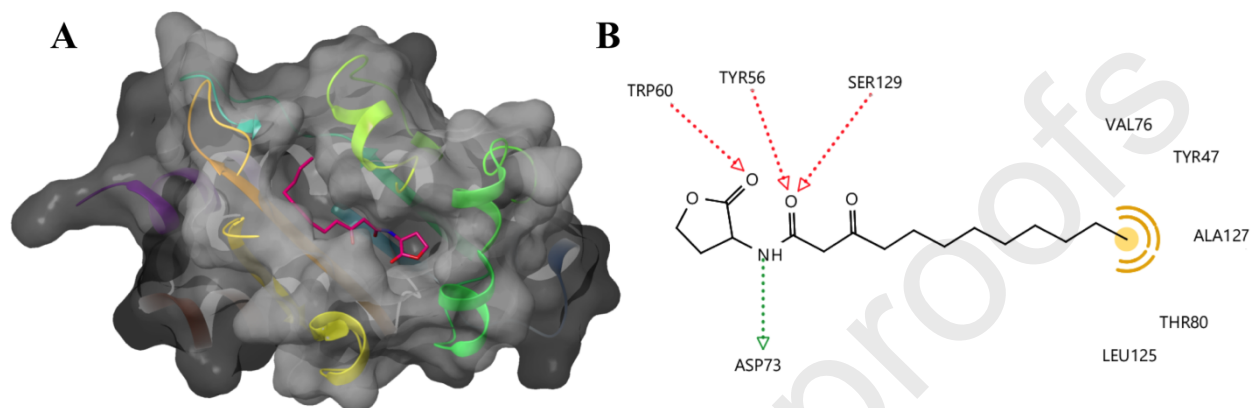


Figure 2. Molecular surface representation of LasR with the co-crystallized ligand ODHL (PDB code: 3IX3) represented as pink stick (A). Identified interaction pattern of ODHL in the active site of LasR (B). Pharmacophoric features are visualized as green arrow (hydrogen bond donor), red arrows (hydrogen bond acceptor), and yellow sphere (hydrophobic interaction).

The urea functionality represents one of the most significant core structures incorporated into organic and medicinal chemistry. This scaffold is inherent to diverse bioactive molecules such as anticancer, antiviral, antibacterial, antihypertensive agents including clinically approved therapeutics (Figure 3) [10].

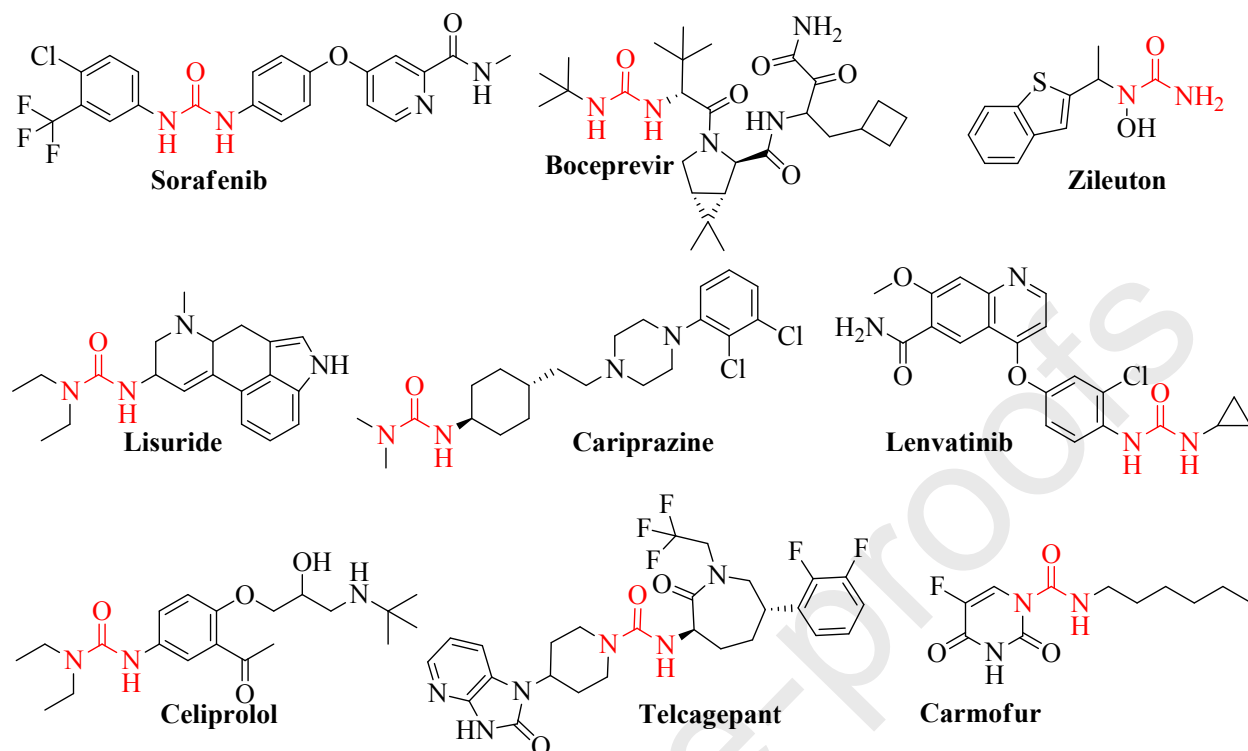


Figure 3. Chemical structures of urea containing FDA approved drug molecules.

Hence, a remarkable amount of researchers focus on the synthesis of different derivatives using urea functionality as an excellent building block. Among them, numerous substituted urea derivatives were reported with their antibacterial, antifungal and antitubercular activities (Figure 4) [11–13].

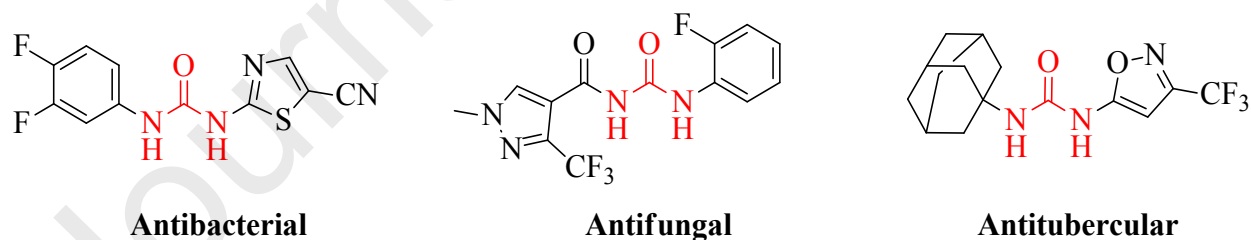


Figure 4. Some examples of disubstituted urea derivatives possessing antimicrobial activities.

Considering the great significance of urea-containing compounds with medicinal purposes as well as different applications of organic reactions or material science, diverse methods have been established for their syntheses [10]. The classical syntheses of urea derivatives include the reaction

of amines with isocyanate, carbamates or phosgene. However, especially due to the high toxicity of phosgene, the researchers focus on finding alternative routes to obtain urea derivatives [14].

Based on the above-mentioned considerations, we aimed to synthesize various substituted urea derivatives and test them against different Gram-positive and Gram-negative bacteria, *Candida albicans* as well as *Mycobacterium tuberculosis*.

2. Results and Discussion

2.1. Chemistry

For the synthesis of the first subseries of the compounds (**U1-U7**), 2-bromo-3-methylpyridine (**II**) was obtained by the bromination reaction of 2-amino-3-methylpyridine (**I**) in the presence of HBr at low temperature. Oxidation of 2-bromo-3-methylpyridine (**II**) with KMnO_4 in the presence of water resulted in the formation of 2-bromonicotinic (**III**) acid. Afterward, 2-bromonicotinic acid was converted into the corresponding azide (**IV**). For this reaction, 2-bromonicotinic was treated with ethyl chloroformate in the presence of triethylamine followed by the addition of a solution of NaN_3 in water. The resulting azide moiety is an excellent starting compound to produce the corresponding isocyanate. Therefore, acyl azide (**IV**) was refluxed in benzene with various amines. Isocyanate was formed in the reaction medium and trapped with amine to give desired urea derivatives **U1-U7** (Figure 5). The structures of the compounds **U1-U7** were elucidated by ^1H NMR, ^{13}C NMR, HRMS and FTIR. ^1H NMR and ^{13}C NMR spectra of the synthesized compounds are provided as supplementary materials.

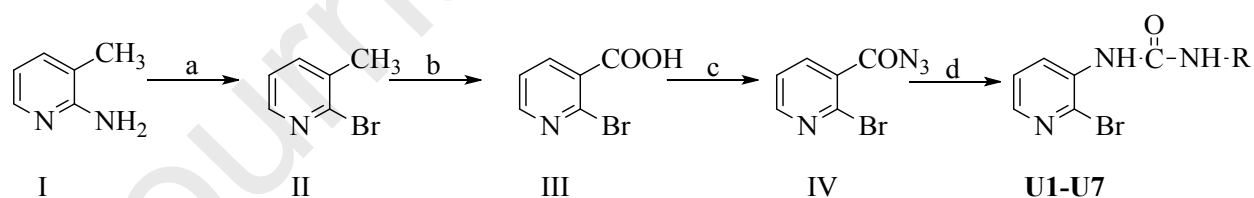


Figure 5. Synthesis of urea derivatives **U1-U7** a) Br_2 , NaNO_2 , 48% HBr, -20°C b) KMnO_4 , H_2O , reflux c) i. Et_3N , ethylchloroformate, THF ii. $\text{NaN}_3/\text{H}_2\text{O}$ d) Substituted amines, benzene, reflux.

Second subseries of the target compounds (**U8-U23**) were synthesized in a simple one-step method. The reaction of 2-aminothiophenol with equivalent amount of various isocyanate derivatives in toluene at 80°C resulted in compounds **U8-U23**. The last derivative **U24** was obtained in DMF at 0°C by the reaction of 2-aminothiophenol with two equivalent amounts of cyclohexyl isocyanate (Figure 6).

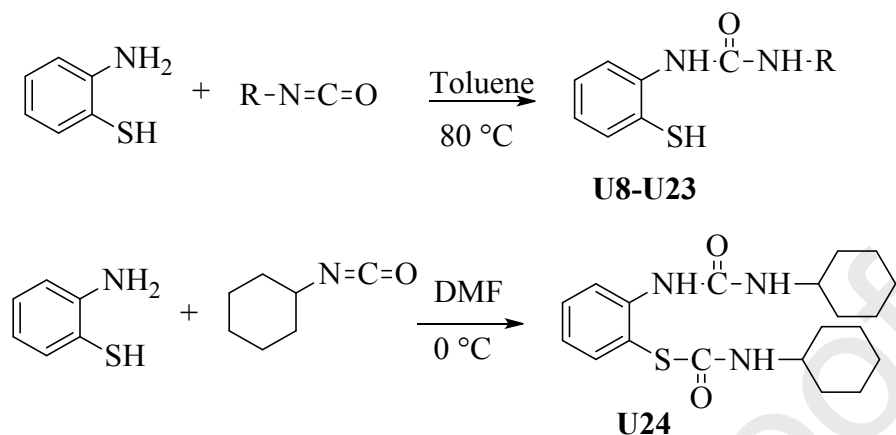
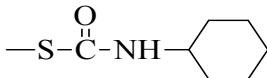


Figure 6. Synthesis of urea derivatives **U8-U24**

The chemical structures of the studied compounds are provided in Table 1.

Table 1. The chemical structures of the tested compounds

Compound	X	R ₁	R ₂
U1	N	Br	phenyl
U2	N	Br	4-methoxyphenyl
U3	N	Br	2-pyridyl
U4	N	Br	2-aminophenyl
U5	N	Br	4-chlorophenyl
U6	N	Br	4-nitrophenyl
U7	N	Br	<i>o</i> -tollylphenyl
U8	C	SH	phenyl

U9	C	SH	4-fluorophenyl
U10	C	SH	4-cyanophenyl
U11	C	SH	4-bromophenyl
U12	C	SH	4-nitrophenyl
U13	C	SH	4-chlorophenyl
U14	C	SH	3-cyanophenyl
U15	C	SH	3,4,5-trimethoxyphenyl
U16	C	SH	4-methoxyphenyl
U17	C	SH	<i>p</i> -tollylphenyl
U18	C	SH	2-naphtyl
U19	C	SH	2,3,4-trimethoxyphenyl
U20	C	SH	3,4-dimethoxyphenyl
U21	C	SH	4-tert-butyl
U22	C	SH	2,4-dimethoxyphenyl
U23	C	SH	<i>o</i> -tollylphenyl
U24	C		cyclohexyl

2.2. Antibacterial and Antifungal Activity Evaluation

The obtained urea derivatives were initially tested for their antibacterial and antifungal activities by determining their minimum inhibitory concentration (MIC) values. Gentamicin, piperacillin-tazobactam and fluconazole were employed as positive control. Table 2 represents the antimicrobial activity of each compound against bacteria and *C. albicans*. The DMSO concentration used to dissolve compounds had no antimicrobial effect.

Table 2. Minimum inhibitory concentrations (MIC) for bacteria and yeast ($\mu\text{g/mL}$)

Compound	Gram-positive bacteria			Gram-negative bacteria		Yeast
	<i>S. aureus</i>	<i>MRSA</i>	<i>E. faecalis</i>	<i>E. coli</i>	<i>P. aeruginosa</i>	<i>C. albicans</i>
	ATCC 29213	ATCC 43300	ATCC 29212	ATCC 25922	ATCC 27853	ATCC 90028
U1	256	256	512	256	256	16
U2	512	256	256	256	256	32
U3	512	256	256	256	512	64
U4	512	512	256	256	512	64
U5	256	512	256	256	256	32
U6	256	512	256	512	512	64
U7	256	256	128	256	256	32
U8	256	128	256	256	64	16
U9	256	256	64	256	128	32
U10	8	16	16	128	2	32
U11	64	64	4	64	32	32
U12	512	512	512	512	512	64
U13	128	128	32	128	128	64
U14	256	256	256	256	32	32
U15	64	64	64	128	0.5	32
U16	256	256	64	512	128	64
U17	256	256	64	512	128	64
U18	128	128	128	512	32	64
U19	256	256	128	256	128	64
U20	256	512	256	256	128	64

U21	256	512	256	256	256	64
U22	256	512	128	256	128	64
U23	256	256	128	256	64	32
U24	128	256	64	256	64	8
Gentamicin	0.06	16	2	0.25	0.25	NA
Piperacillin/ Tazobactam	0.125	NA	0.25	0.25	0.25	NA
Fluconazole	NA	NA	NA	NA	NA	0.125

NA: Not applicable.

According to the obtained results, the synthesized derivatives possessed antimicrobial activity with MIC values ranging between 0.5 and 512 $\mu\text{g/mL}$ against all tested microorganisms. It is noteworthy to mention that **U15** was the most active compound on *P. aeruginosa* with a MIC value of 0.5 $\mu\text{g/mL}$. Furthermore, **U10** was one of the most attractive compounds effective on *P. aeruginosa* and *S. aureus* with MIC of 2 and 8 $\mu\text{g/mL}$, respectively. Additionally, **U11** showed high antimicrobial activity against *E. faecalis* possessing MIC of 4 $\mu\text{g/mL}$. **U24** stands as the most active compound as antifungal agent against *C. albicans* with 8 $\mu\text{g/mL}$ MIC value.

When the obtained results are evaluated out in terms of the chemical structures of the compounds, the substitution of the urea moiety with 2-bromopyridine ring (**U1-U7**) did not lead to an improvement in the antimicrobial activity. It is interesting to note that all active compounds (**U10**, **U11** and **U15**) belong to the second subseries carrying 2-mercaptophenyl ring. Additionally, the most effective antibacterial compound (**U15**) carries three methoxy groups on the 3'-phenyl ring. **U24**, which has the lowest MIC value on *C. albicans*, is considered to be the most active antifungal agent among all compounds. At the same time, it is the only compound carrying a bulky substituent on the thiol group of the phenyl ring. Consequently, antifungal activity can be related to the increased lipophilicity of **U24**.

2.3. Antitubercular Activity Evaluation

All synthesized urea derivatives were evaluated for their antitubercular activities against *M. tuberculosis* H₃₇Rv utilizing Microplate Alamar Blue Assay (MABA) method. Isoniazid, rifampicin, and ethambutol were used as reference compounds. The antimycobacterial activity screening results are reported as MIC values in Table 3.

Table 3. Antitubercular activities of the compounds

Compound	MIC (µg/mL)	Compound	MIC (µg/mL)
U1	>25	U13	25
U2	25	U14	>25
U3	>25	U15	>25
U4	>25	U16	>25
U5	25	U17	>25
U6	>25	U18	>25
U7	>25	U19	>25
U8	>25	U20	>25
U9	>25	U21	>25
U10	12.5	U22	>25
U11	>25	U23	>25
U12	>25	U24	6.25
isoniazid: 0.05, Rifampicin: 0.1, Ethambutol: 1.56			

The obtained MIC values revealed that **U2**, **U5** and **U13** were moderate inhibitors of *M. tuberculosis* with MIC value of 25 µg/mL. Among the compounds, **U10** and **U24** were found to be more active on *M. tuberculosis* showing 6.25 and 12.5 µg/mL MIC values, respectively. It is remarkable that **U24**, the only active compound as antifungal agent, was found to be the best inhibitor of *M. tuberculosis* growth inhibition at the same time.

2.4. Structure-Activity Relationship

According to the data obtained from biological activity determination experiments, we summarized the structural requirements of the compounds possessing antimicrobial activities in Figure 7.

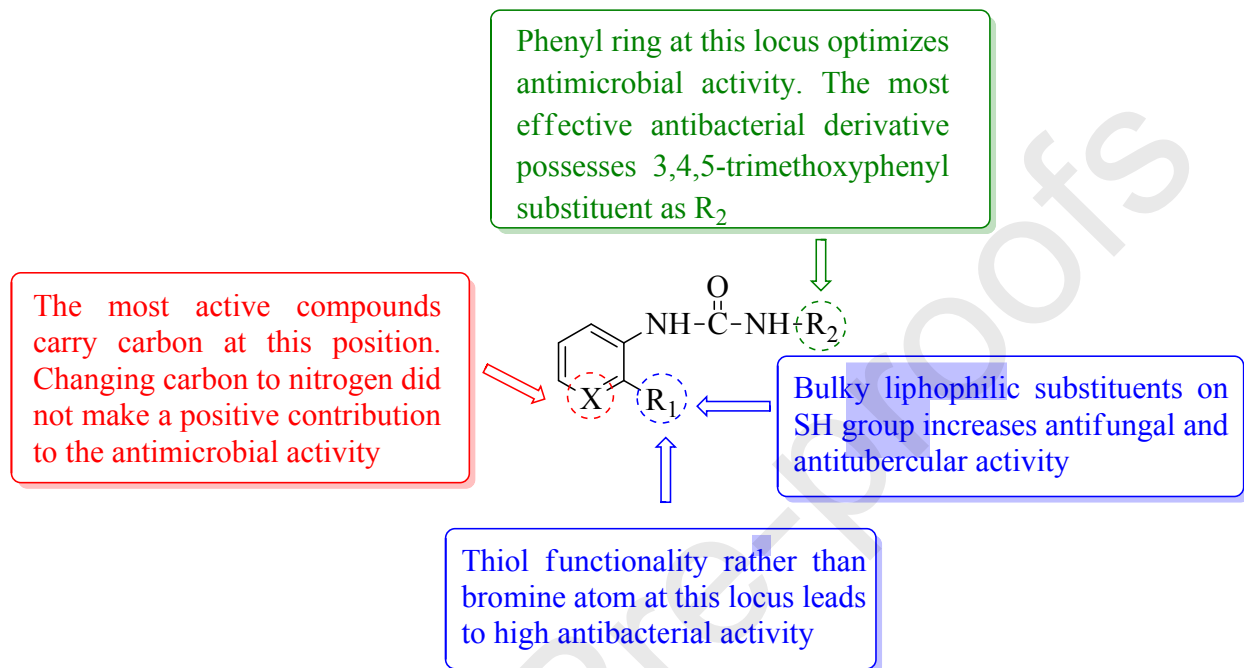


Figure 7. Structure-activity relationships of the synthesized compounds

2.5. *In-vitro* Biofilm Inhibition

Among the tested compounds, **U10** and **U15** showed strong antibacterial activity against *P. aeruginosa*. Moreover, the antimicrobial activity of **U15** seems to be specific to *P. aeruginosa* since its MIC values against other tested bacteria were relatively higher. Thus, we mainly focused on these two compounds for further biofilm inhibition assay.

The MIC concentrations of **U10** and **U15** against PAO1 were 4 $\mu\text{g/mL}$ and 1 $\mu\text{g/mL}$, respectively. Thus we used MIC, MIC/2 and MIC/4 concentrations for each compound. Both inhibitory and sub-inhibitory concentrations for **U10** lead to a significant decrease in PAO1 biofilm formation when compared to control. The percentage of biofilm inhibition was as follows: 56.83% for MIC, 48.92% for MIC/2, 29.50% for MIC/4. **U15** showed a diminished anti-biofilm effect when compared to **U10**. However, both MIC and MIC/2 concentrations were significantly decreased PAO1 biofilm formation (30.22% and 20.14% decrease, respectively) (Figure 8)

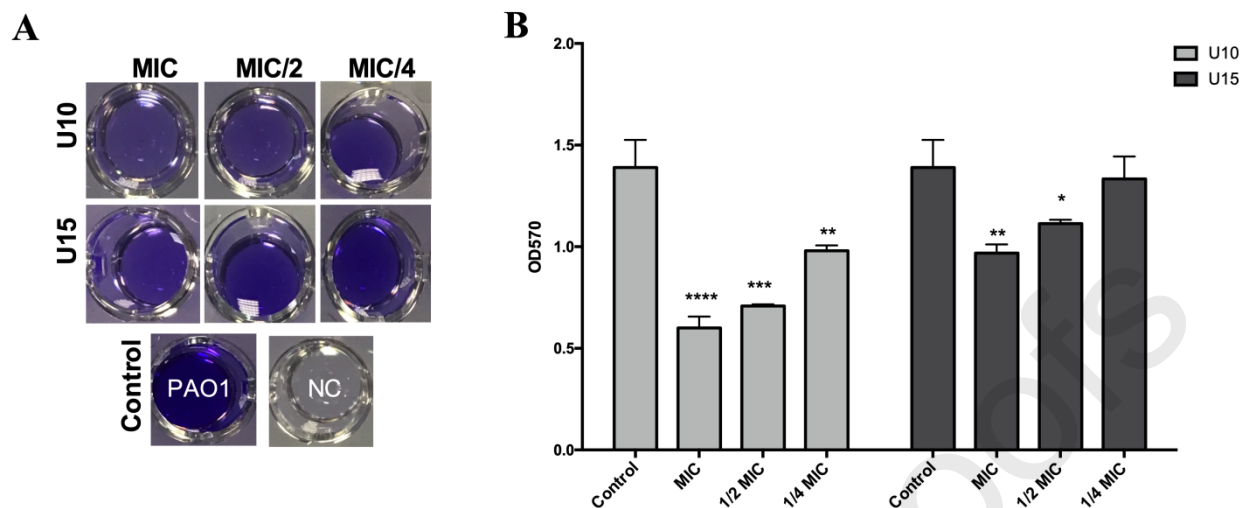


Figure 8. In-vitro biofilm inhibition assay. A) Representative pictures for crystal violet staining microtiter biofilm formation assay (Control wells; PAO1 alone and NC:Negative control) B) Inhibitory effect of MIC, MIC/2 and MIC/4 values of **U10** and **U15** against PAO1 biofilms, which were quantified by crystal violet staining. *P. aeruginosa* PAO1 alone was used as control. Statistical comparisons were made between each group and control mean OD570 value by using two-way ANOVA; * $p < 0.05$, ** $p < 0.01$, *** $p < 0.001$, **** $p < 0.0001$.

2.6. Molecular Docking

Biofilm formation is directly quorum sensing-controlled mechanism in bacteria. Therefore, inhibiting QS in *P. aeruginosa* decreases biofilm formation. Besides, it is a rational and frequently used approach to mimic the signal molecules by using analog synthetic compounds for QS inhibition. Therefore, we aimed to explain the activities of **U10** and **U15** by molecular docking studies. To investigate the anti-biofilm activity mechanism of **U10** and **U15**, we initially examined the binding interactions of N-3-(oxododecanoyl)-L-homoserine lactone, 3-oxo-N-(2-oxotetrahydrofuran-3-yl)octanamide, (ODHL) which is a co-crystallized ligand in LasR binding site. This compound binds to LasR via four key hydrogen bonds and hydrophobic interactions. The carbonyl group of lactone moiety and the amide functionality are responsible for forming these hydrogen bonds. The long alkyl side chain occupies the hydrophobic pocket. The structural requirements of ODHL to regulate QS in *P. aeruginosa* and the overlaid docking poses of **U10** and **U15** within LasR active site are provided in Figure 9.

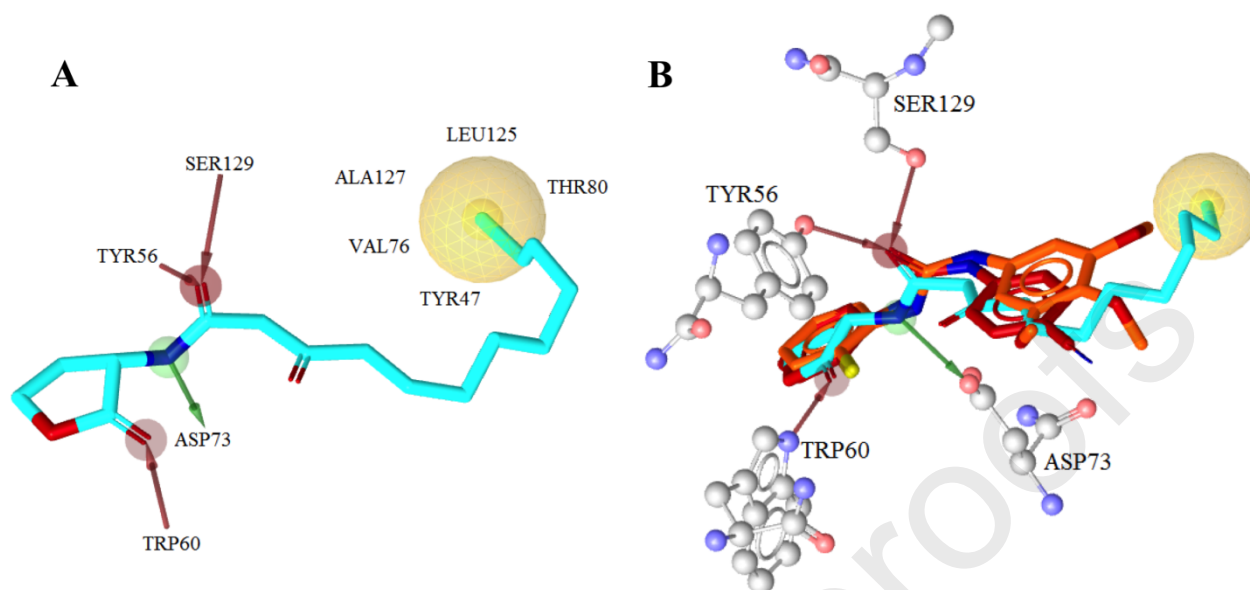


Figure 9. Identified pharmacophores of ODHL in LasR binding site (A). Superimposition of ODHL (cyan stick), **U10** (red stick) and **U15** (orange stick) after docking to the active pocket of LasR (B). Red arrow - hydrogen bond acceptor, green arrow - hydrogen bond donor, yellow sphere - hydrophobic interaction

Figure 10 reports the detailed binding interactions of **U10** and **U15** in the active site of LasR, the transcriptional regulator of QS. When the plausible binding modes of these compounds in the active pocket of LasR were analyzed, it was observed that the urea functionality, the core scaffold, formed three key hydrogen-bonding interactions to Tyr56, Asp73 and Ser129 in the same manner as the amide functionality of ODHL. Additionally, thiol group in **U10** and **U15** served as a hydrogen bond acceptor like the carbonyl of the lactone moiety in the original ligand. Also, phenyl rings of the test compounds were responsible for the further hydrophobic contacts. The lack of a long alkyl side chain in **U10** and **U15** leads to loss of the interaction in the hydrophobic pocket of LasR, where the original ligand interacts to activate QS. In this manner, our compounds are stabilized in the binding site by hydrogen bonds but cannot behave like an activator. The number of increased hydrophobic contacts in **U10** with LasR explains the higher biofilm inhibition capacity compared to **U15**. Consequently, with these pharmacophore similarities between our compounds and ODHL, **U10** and **U15** are likely to inhibit LasR activation and act as QS and biofilm inhibitors in *P. aeruginosa*. Although our in-silico studies indicate this potential mechanism of action in decreasing biofilm formation, further mechanistic studies to confirm their direct interaction with QS signal receptors will shed light on this issue.

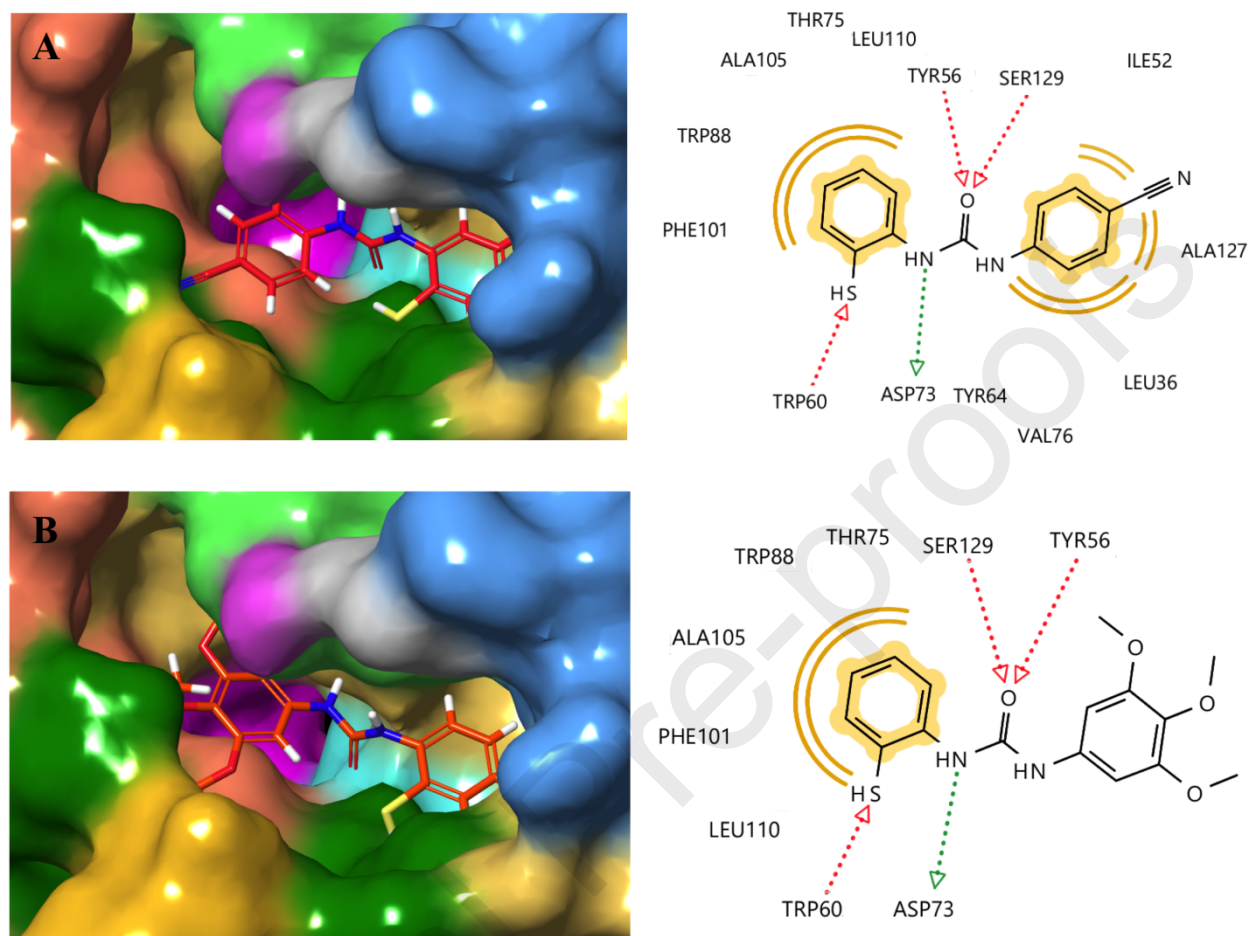


Figure 10. Proposed docking poses of **U10** (A) and **U15** (B) in the binding site LasR and 2D depictions of the formed interactions. Red arrow - hydrogen bond acceptor, green arrow - hydrogen bond donor, yellow sphere - hydrophobic interaction

2.7. *In Silico* Prediction of Physicochemical Properties of Active Molecules

Some bioactive molecules may be unsuccessful to turn into good drug molecules because of their unsuitable physicochemical properties. Therefore, it is a useful approach to predict the molecular properties of novel drug candidates. Here, we carried out computational calculations to foresee the parameters of the most active antimicrobial compounds and to determine their drug-likeness properties (Table 4).

Lipinski's rule of five [15] is applied to estimate drug-likeness and clarify the essential molecular descriptors which are important to predict the oral bioavailability and cell permeability of new bioactive molecules. Along with its descriptors, we also calculated the number of rotatable bonds

(nROTB) and topological polar surface area (TPSA), which are accepted to be important parameters to determine the oral bioavailability of drug molecules [16].

Table 4. Calculated molecular properties of the most active molecules

Compound	LogP ^[a]	M.W. ^[b]	HBA ^[c]	HBD ^[d]	TPSA ^[e]	nROTB ^[f]	%ABS	Lipinski's Violation
U10	3.08	269.33	4	2	64.92	2	86.60	0
U11	4.13	323.21	3	2	41.12	2	94.81	0
U15	2.96	334.40	6	2	68.83	5	85.25	0
U24	5.29	375.54	5	3	70.22	5	84.77	1

^aLogP: logarithm of *n*-octanol-water partition coefficient

^bM.W: molecular weight

^cHBA: number of hydrogen bond acceptors

^dHBD: number of hydrogen bond donors

^eTPSA: topological polar surface area

^fnROTB: number of rotatable bonds

According to the calculated parameters, three of the compounds completely adhere to Lipinski's rule of five. Only **U24** presented a slight violation with its LogP value. However, this value does not exceed the accepted range excessively. Also, the increased lipophilicity can be a determining factor for its high activity against *M. tuberculosis* and *C. albicans* compared to the other tested compounds. TPSA values of the compounds were found to be ranging between 41.12 and 70.22, which is an acceptable range considering that this value is below 140-150 Å² for the most known drug molecules. TPSA was also used to calculate the percentage of absorption using this equation: %ABS=109-0.345xTPSA and the rates were found to be good for intestinal absorption. The number of rotatable bonds is an important parameter that indicates molecular flexibility. To restrict the conformational changes while interacting with the biological target, this value should be ≤ 10. All of our active compounds have less than ten rotatable bonds.

Consequently, these compounds exhibit excellent physicochemical properties to serve as antimicrobial drug candidates [17].

3. Conclusion

In this study, we synthesized and tested 1,3-disubstituted urea derivatives for their antimicrobial activities. In addition to the classical urea synthesis, we reported a new route to convert methyl

group to substituted urea functionality. Extensive antimicrobial tests on bacterial strains, *C. albicans* and *M.tuberculosis* resulted in new potential molecules against bacterial, fungal and tubercular infections. The obtained results indicated that introducing 2-mercaptophenyl ring into the core urea functionality led to an improvement in the antibacterial activities of the compounds. Substitution of the thiol group with a bulky group increased the lipophilicity of the compounds and provided better antifungal and antitubercular activities. Also, we carried out further studies on two molecules, active on *P. aeruginosa*, via determining their biofilm inhibition capacities. According to the obtained data from molecular docking studies, these compounds are likely to decrease biofilm formation via quorum sensing inhibition. Calculated parameters of the most active compounds showed that these compounds can be considered as drug candidates. Consequently, our findings can be useful for the discovery of future molecules for the successful treatment of the antimicrobial infections.

4. Experimental

4.1. Chemistry

4.1.2. Materials and Methods

Toluene and benzene were distilled from sodium-benzophenone just prior to use. All reagents were commercially purchased and used without further purification. All reactions were monitored by TLC performed on pre-coated 60 F254 plates. Visualization was effected with UV using Camag Thin-Layer Chromatogram Lamp (254/366 nm). Melting points were determined using open glass capillaries and are uncorrected. Infrared (IR) spectra were recorded in the range 4000–600 cm^{-1} via ATR diamond. ^1H NMR and ^{13}C NMR spectra were determined under ambient temperature conditions in DMSO-*d*₆ solution using a Bruker AM 400 MHz spectrophotometer. The chemical shifts (δ) were reported in parts per million (ppm) and were relative to the central peak of the solvent, which was DMSO-*d*₆. MS spectra were carried out on an LC/MS High-Resolution Time of Flight (TOF) Agilent 1200/6530 instrument at the Atatürk University-East Anatolian High Technology Research and Application Center (DAYTAM).

4.1.3. General procedure for the synthesis of urea derivatives U1-U7

To a solution of 2-bromonicotinic acid [18–20] (0.5 g, 2.48 mmol) in 10 mL THF at -5 °C, triethylamine (0.36 mL, 2.48 mmol) in THF (5 mL) was added dropwise and the resulting mixture was stirred for 30 min. Cooled solution of ethyl chloroformate (0.31 mL, 2.98 mmol) in THF (5 mL) was added to the reaction mixture at the same temperature. After additional stirring for 30 min., a solution of sodium azide (0.32 g, 4.96 mmol) in water (5 mL) was added dropwise. The reaction mixture was stirred at room temperature for 18h-24h. The mixture was extracted with ethyl acetate (3×15 mL) and the organic phase was washed with saturated sodium bicarbonate (3×30 mL) and with water (2×25 mL) and dried over MgSO₄. After the removal of ethyl acetate, azide (0.41 g, 73%) was obtained as white solid. The obtained azide was used the next step without any purification process. Acyl azide and one equimolar amine were heated at reflux in freshly distilled benzene (10 mL) for 18-24h. The formed precipitate was filtered and washed with benzene to give pure samples **U1-U7**.

1-(2-Bromopyridin-3-yl)-3-phenylurea (U1)

White solid, yield: 39%. mp 170-172 °C; R_f (EtOAc:Hexane=1:1):0.55; IR (ATR) 3270, 3065, 1636, 1549, 1391, 1203, 1043. ¹H NMR (400 MHz, DMSO) δ 9.59 (s, 1H, -NH), 8.42 (dd, *J* = 8.2, 1.8 Hz, 1H), 8.27 (s, 1H, -NH), 8.03 (dd, *J* = 4.5, 1.8 Hz, 1H), 7.49 – 7.44 (m, 2H), 7.41 (dd, *J* = 8.1, 4.5 Hz, 1H), 7.34 – 7.26 (m, 2H), 7.01 (t, *J* = 7.4 Hz, 1H). ¹³C NMR (100 MHz, DMSO) δ 152.43, 143.77, 139.59, 135.35, 133.07, 129.60, 129.42, 124.12, 122.87, 118.75. HRMS (EI): [M+H]⁺, found 292.0069. C₁₂H₁₁BrN₃O requires 292.0085.

1-(2-Bromopyridin-3-yl)-3-(4-methoxyphenyl)urea (U2)

White solid, yield: 24%. mp 170-171 °C; R_f (EtOAc:Hexane=1:1):0.47; IR (ATR) 3663, 2987, 2906, 1708, 1623, 1517, 1384, 1231. ¹H NMR (400 MHz, DMSO) δ 9.41 (s, 1H, -NH), 8.41 (dd, *J* = 8.2, 1.9 Hz, 1H), 8.17 (s, 1H, -NH), 8.01 (dd, *J* = 4.6, 1.9 Hz, 1H), 7.54 – 7.25 (m, 3H), 7.01 – 6.81 (m, 2H), 3.71 (s, 3H). ¹³C NMR (100 MHz, DMSO) δ 155.26, 152.54, 143.56, 135.49, 132.90, 132.52, 129.39, 124.10, 120.58, 114.57, 55.62. HRMS (EI): [M+H]⁺, found 322.0193. C₁₃H₁₃BrN₃O₂ requires 322.0191.

1-(2-Bromopyridin-3-yl)-3-(pyridin-2-yl)urea (U3)

White solid, yield: 53%. mp 227-228 °C; R_f (EtOAc:Hexane=1:1):0.46; IR (ATR) 2976, 1696, 1578, 1532, 1475, 1307, 1238. ^1H NMR (400 MHz, DMSO) δ 12.16 (s, 1H), 10.17 (s, 1H), 8.64 (d, $J = 8.2$ Hz, 1H), 8.35 (d, $J = 4.4$ Hz, 1H), 8.06 (dd, $J = 4.5, 1.7$ Hz, 1H), 7.92 – 7.74 (m, 1H), 7.43 (dd, $J = 8.2, 4.5$ Hz, 1H), 7.18 (bd, $J = 8.3$ Hz, 1H), 7.06 (dd, $J = 7.2, 5.1$ Hz, 1H). ^{13}C NMR (100 MHz, DMSO) δ 152.92, 152.71, 146.72, 143.84, 139.63, 135.73, 132.88, 128.97, 124.14, 118.17, 112.47. HRMS (EI): $[\text{M}+\text{H}]^+$, found 293.0014. $\text{C}_{11}\text{H}_{10}\text{BrN}_4\text{O}$ requires 293.1320.

1-(2-Aminophenyl)-3-(2-bromopyridin-3-yl)urea (U4)

White solid, yield: 42%. mp 170-172 °C; R_f (EtOAc:Hexane=1:1):0.55; IR (ATR) 3662, 2987, 2900, 1619, 1531, 1384, 1249, 1051. ^1H NMR (400 MHz, DMSO) δ 8.67 (s, 1H, -NH), 8.45 (dd, $J = 8.3, 1.9$ Hz, 1H), 8.31 (s, 1H, -NH), 8.00 (dd, $J = 4.5, 1.8$ Hz, 1H), 7.41 – 7.35 (m, 1H), 7.29 (dd, $J = 7.9, 1.5$ Hz, 1H), 6.87 (td, $J = 7.7, 1.6$ Hz, 1H), 6.77 – 6.72 (m, 1H), 6.56 (td, $J = 7.6, 1.6$ Hz, 1H), 4.87 (s, 2H). ^{13}C NMR (100 MHz, DMSO) δ 153.18, 143.36, 142.03, 135.76, 132.62, 129.15, 125.70, 125.05, 124.09, 123.92, 117.02, 116.18. HRMS (EI): $[\text{M}+\text{H}]^+$, found 307.0186. $\text{C}_{12}\text{H}_{12}\text{BrN}_4\text{O}$ requires 307.0194.

1-(2-Bromopyridin-3-yl)-3-(4-chlorophenyl)urea (U5)

White solid, yield: 39%. mp 232-234 °C; R_f (EtOAc:Hexane=1:1):0.53; IR (ATR) 3280, 3200, 1637, 1592, 1572, 1544, 1390, 1243, 1203, 1049. ^1H NMR (400 MHz, DMSO) δ 9.71 (s, 1H, -NH), 8.39 (dd, $J = 8.2, 1.9$ Hz, 1H), 8.29 (s, 1H, -NH), 8.04 (dd, $J = 4.6, 1.8$ Hz, 1H), 7.53 – 7.45 (m, 2H), 7.41 (dd, $J = 8.2, 4.6$ Hz, 1H), 7.38 – 7.32 (m, 2H). ^{13}C NMR (100 MHz, DMSO) δ 152.37, 144.00, 138.57, 135.16, 133.27, 129.80, 129.27, 126.39, 124.14, 120.29. HRMS (EI): $[\text{M}+\text{H}]^+$, found 325.9696. $\text{C}_{12}\text{H}_{10}\text{BrClN}_3\text{O}$ requires 325.9693.

1-(2-Bromopyridin-3-yl)-3-(4-nitrophenyl)urea (U6)

Yellow solid, yield: 58%. mp 254-256 °C; R_f (EtOAc:Hexane=1:1):0.47; IR (ATR) 3451, 3273, 1722, 1650, 1573, 1507, 1325, 1177, 1107. ^1H NMR (400 MHz, DMSO) δ 10.30 (s, 1H, -NH), 8.54 (s, 1H, -NH), 8.37 (d, $J = 8.3$ Hz, 1H), 8.20 (d, $J = 9.0$ Hz, 2H), 8.08 (d, $J = 4.9$ Hz, 1H), 7.70 (d, $J = 9.2$ Hz, 2H), 7.52 – 7.29 (m, 1H). ^{13}C NMR (100 MHz, DMSO) δ 152.20, 145.96, 144.79, 141.95, 134.56, 133.96, 130.78, 125.65, 124.23, 118.26. HRMS (EI): $[\text{M}+\text{H}]^+$, found 336.9942. $\text{C}_{12}\text{H}_{10}\text{BrN}_4\text{O}_3$ requires 336.9936.

1-(2-Bromopyridin-3-yl)-3-(*o*-tolyl)urea (U7)

White solid, yield: 62%. mp 234-235 °C; R_f (EtOAc:Hexane=1:1):0.61; IR (ATR) 2977, 1697, 1533, 1475, 1420, 1307, 1238. ^1H NMR (400 MHz, DMSO) δ 8.78 (s, 1H), 8.62 (s, 1H), 8.37 (d, $J = 8.2$ Hz, 1H), 8.21 – 7.94 (m, 1H), 7.72 (d, $J = 8.3$ Hz, 1H), 7.40 (dd, $J = 8.1, 4.5$ Hz, 1H), 7.28 – 7.11 (m, 2H), 6.99 (t, $J = 7.5$ Hz, 1H), 2.26 (s, 3H). ^{13}C NMR (100 MHz, DMSO) δ 152.89, 143.81, 137.15, 135.55, 133.23, 130.78, 130.21, 129.12, 126.61, 124.04, 123.99, 122.70, 18.52. HRMS (EI): $[\text{M}+\text{H}]^+$, found 306.0263. $\text{C}_{12}\text{H}_{13}\text{BrN}_3\text{O}$ requires 306.0242.

4.1.4. General procedure for the synthesis of urea derivatives U8-U23

U8-U23 were synthesized according to the reported literature procedure [21]. Briefly, they are obtained by the reaction of 2-aminothiophenole and corresponding phenyl isocyanate derivatives in dry toluene. The resulting residue obtained upon the completion of the reaction was purified by crystallization from ethanol to afford the target compounds **U8-U23**. These compounds were included in this study as their biological activities were not studied before.

1-(2-Mercaptophenyl)-3-phenylurea (U8) ^1H NMR (400 MHz, DMSO) δ 9.36 (s, 1H), 8.39 (s, 1H), 7.96 (d, $J = 8.0$ Hz, 1H), 7.46 (d, $J = 7.5$ Hz, 2H), 7.38 – 7.18 (m, 4H), 7.07 – 6.78 (m, 2H).

1-(4-Fluorophenyl)-3-(2-mercaptophenyl)urea (U9) ^1H NMR (400 MHz, DMSO) δ 9.39 (s, 1H), 8.37 (s, 1H), 7.94 (d, $J = 8.0$ Hz, 1H), 7.49–7.40 (m, 2H), 7.31 (dd, $J = 16.5, 7.5$ Hz, 2H), 7.14 (dd, $J = 12.0, 5.5$ Hz, 2H), 6.95 (td, $J = 7.5, 1.0$ Hz, 1H).

1-(4-Cyanophenyl)-3-(2-mercaptophenyl)urea (U10) ^1H NMR (400 MHz, DMSO) δ 9.81 (s, 1H), 8.55 (s, 1H), 7.90 (d, $J = 8.0$ Hz, 1H), 7.75 (d, $J = 8.5$ Hz, 2H), 7.62 (d, $J = 8.5$ Hz, 2H), 7.38 (d, $J = 7.5$ Hz, 1H), 7.29 (t, $J = 7.0$ Hz, 1H), 7.00 (t, $J = 7.5$ Hz, 1H).

1-(4-Bromophenyl)-3-(2-mercaptophenyl)urea (U11) ^1H NMR (400 MHz, DMSO) δ 9.48 (s, 1H), 8.41 (s, 1H), 7.92 (d, $J = 8.2$ Hz, 1H), 7.49 – 7.39 (m, 4H), 7.34 (dd, $J = 7.5, 1.0$ Hz, 1H), 7.29 (t, $J = 7.5$ Hz, 1H), 6.96 (td, $J = 7.5, 1.0$ Hz, 1H).

1-(2-Mercaptophenyl)-3-(4-nitrophenyl)urea (U12) ^1H NMR (400 MHz, DMSO) δ 10.02 (s, 1H), 8.60 (s, 1H), 8.20 (d, $J = 9.0$ Hz, 2H), 7.91 (d, $J = 8.0$ Hz, 1H), 7.67 (d, $J = 9.0$ Hz, 2H), 7.39 (d, $J = 7.5$ Hz, 1H), 7.30 (t, $J = 7.5$ Hz, 1H), 7.01 (t, $J = 7.0$ Hz, 1H).

1-(4-Chlorophenyl)-3-(2-mercaptophenyl)urea (U13) ^1H NMR (400 MHz, DMSO) δ 9.49 (s, 1H), 8.41 (s, 1H), 7.92 (d, $J = 8.0$ Hz, 1H), 7.47 (d, $J = 9.0$ Hz, 2H), 7.38 – 7.24 (m, 4H), 6.96 (t, $J = 7.5$ Hz, 1H).

1-(3-Cyanophenyl)-3-(2-mercaptophenyl)urea (U14) ^1H NMR (400MHz, DMSO) δ 9.67 (s, 1H), 8.51 (s, 1H), 7.98 (s, 1H), 7.90 (d, $J = 7.5$ Hz, 1H), 7.63 (d, $J = 7.5$ Hz, 1H), 7.50 (t, $J = 8.0$ Hz, 1H), 7.44 (d, $J = 7.5$ Hz, 1H), 7.37 (d, $J = 8.0$ Hz, 1H), 7.30 (t, $J = 7.5$ Hz, 1H), 6.99 (t, $J = 7.0$ Hz, 1H).

1-(2-Mercaptophenyl)-3-(3,4,5-trimethoxyphenyl)urea (U15) ^1H NMR (400 MHz, DMSO) δ 9.37 (s, 1H), 8.36 (s, 1H), 7.98 (d, $J = 8.0$ Hz, 1H), 7.30 (d, $J = 7.5$ Hz, 2H), 6.95 (t, $J = 7.5$ Hz, 1H), 6.80 (s, 2H), 3.75 (s, 6H), 3.61 (s, 3H).

1-(2-Mercaptophenyl)-3-(4-methoxyphenyl)urea (U16) ^1H NMR (400 MHz, DMSO) δ 9.20 (s, 1H), 8.31 (s, 1H), 7.97 (d, $J = 8.5$ Hz, 1H), 7.36 (d, $J = 8.5$ Hz, 2H), 7.30 (d, $J = 7.5$ Hz, 2H), 6.93 (t, $J = 7.5$ Hz, 1H), 6.88 (d, $J = 8.5$ Hz, 2H), 3.71 (s, 3H).

1-(2-Mercaptophenyl)-3-(*p*-tolyl)urea (U17) ^1H NMR (400 MHz, DMSO) δ 9.27 (s, 1H), 8.35 (s, 1H), 7.96 (d, $J = 8.0$ Hz, 1H), 7.42 – 7.18 (m, 4H), 7.10 (d, $J = 7.5$ Hz, 2H), 6.94 (t, $J = 7.0$ Hz, 1H), 2.25 (s, 3H).

1-(2-Mercaptophenyl)-3-(naphthalen-2-yl)urea (U18) ^1H NMR (400 MHz, DMSO) δ 9.39 (s, 1H), 8.86 (s, 1H), 8.18 (d, $J = 8.0$ Hz, 1H), 8.00 (d, $J = 8.0$ Hz, 1H), 7.95 (t, $J = 7.0$ Hz, 2H), 7.67 (d, $J = 8.0$ Hz, 1H), 7.63 – 7.51 (m, 2H), 7.48 (t, $J = 7.5$ Hz, 1H), 7.42 (d, $J = 7.5$ Hz, 1H), 7.32 (t, $J = 7.5$ Hz, 1H), 7.00 (t, $J = 7.5$ Hz, 1H).

1-(2-Mercaptophenyl)-3-(2,3,4-trimethoxyphenyl)urea (U19) ^1H NMR (400 MHz, DMSO) δ 8.87 (s, 1H), 8.73 (s, 1H), 7.79 (d, $J = 8.0$ Hz, 1H), 7.71 (d, $J = 9.0$ Hz, 1H), 7.41 (dd, $J = 7.5, 1.0$ Hz, 1H), 7.29 (t, $J = 7.5$ Hz, 1H), 7.01 (t, $J = 7.5$ Hz, 1H), 6.73 (d, $J = 9.0$ Hz, 1H), 3.80 (s, 3H), 3.77 (s, 3H), 3.75 (s, 3H).

1-(3,4-Dimethoxyphenyl)-3-(2-mercaptophenyl)urea (U20) ^1H NMR (400 MHz, DMSO) δ 9.26 (s, 1H), 8.32 (s, 1H), 7.98 (d, $J = 8.0$ Hz, 1H), 7.37 – 7.24 (m, 2H), 7.17 (d, $J = 1.5$ Hz, 1H), 7.03 – 6.73 (m, 3H), 3.73 (s, 3H), 3.70 (s, 3H).

1-(Tert-butyl)-3-(2-mercaptophenyl)urea (U21) ^1H NMR (400 MHz, DMSO) δ 7.93 (d, $J = 8.0$ Hz, 1H), 7.90 (s, 1H), 7.25 (dd, $J = 14.0, 7.0$ Hz, 2H), 6.91 – 6.78 (m, 3H), 1.29 (s, 9H).

1-(2,4-Dimethoxyphenyl)-3-(2-mercaptophenyl)urea (U22) ^1H NMR (400 MHz, DMSO) δ 8.79 (s, 1H), 8.61 (s, 1H), 7.82 (t, $J = 9.0$ Hz, 2H), 7.39 (d, $J = 7.5$ Hz, 1H), 7.28 (t, $J = 7.5$ Hz, 1H), 6.99 (t, $J = 7.0$ Hz, 1H), 6.61 (d, $J = 2.5$ Hz, 1H), 6.47 (dd, $J = 8.5, 2.5$ Hz, 1H), 3.85 (s, 3H), 3.73 (s, 3H).

1-(2-Mercaptophenyl)-3-(*o*-tolyl)urea (U23) ^1H NMR (400 MHz, DMSO) δ 9.31 (s, 1H), 8.38 (s, 1H), 7.96 (d, $J = 8.0$ Hz, 1H), 7.35 – 7.27 (m, 3H), 7.24 (d, $J = 8.0$ Hz, 1H), 7.17 (t, $J = 7.5$ Hz, 1H), 6.95 (t, $J = 7.5$ Hz, 1H), 6.80 (d, $J = 7.0$ Hz, 1H), 2.28 (s, 3H).

4.1.5. General procedure for the synthesis of urea derivative U24

S-(2-(3-cyclohexylureido)phenyl) cyclohexylcarbamothioate (**U24**) was synthesized according to the modified literature procedure [22]. 2-Aminothiophenol was reacted with two equimolar amounts of cyclohexyl isocyanate solution in DMF. The resulting residue was purified by crystallization from Et_2O to afford **U24**. ^1H NMR (400 MHz, DMSO- d_6) δ 8.17 (d, $J = 7.5$ Hz, 1H), 8.11 (d, $J = 8.3$ Hz, 1H), 7.81 (s, 1H), 7.39 – 7.25 (m, 2H), 7.12 (d, $J = 7.6$ Hz, 1H), 6.90 (t, $J = 7.5$ Hz, 1H), 3.54 – 3.39 (m, 2H), 1.88 – 1.47 (m, 10H), 1.38 – 0.96 (m, 10H).

4.2. Determination of Antimicrobial Activity by Broth Microdilution

The minimum inhibitory concentrations (MIC) of the compounds were determined by broth microdilution method according to the Clinical and Laboratory Standards Institute (CLSI) recommendations [23,24]. Antibacterial activity testing was carried out with *Staphylococcus aureus* ATCC 29213, *Enterococcus faecalis* ATCC 29212, methicillin resistant *Staphylococcus aureus* ATCC 43300, *Escherichia coli* ATCC 25922, *Pseudomonas aeruginosa* ATCC 27853 and antifungal activity was tested against *C. albicans* ATCC 90028. The stock solutions of the compounds were prepared by dissolving in dimethyl sulphoxide (DMSO). MIC was defined as the lowest concentration of the samples with no bacterial growth.

4.3. Microplate Alamar Blue Assay for *Mycobacterium tuberculosis*

The minimum inhibitory concentrations (MIC) of the synthesized compounds were tested using *in-vitro* MABA (Microplate Alamar Blue Assay) assay applying the reported protocol [17]. Assay was performed in duplicate for each compound and the interpretations were compared to standard TB drugs isoniazid, rifampicin and ethambutol. Bacterial growth was observed by colour change and the minimum concentration that didn't change the colour was taken as its MIC value.

4.4. *In-vitro* Biofilm Inhibition Assay

We used biofilm positive laboratory strain of *P. aeruginosa* PAO1 for biofilm experiments. *In-vitro* biofilm inhibition assay was performed as previously described with slight modifications [26]. MIC of compounds **U10** and **U15** against PAO1 was determined with broth microdilution method as described above. MIC, MIC/2, MIC/4 concentrations for each compound were used for crystal violet staining microtiter biofilm formation assay. Briefly, each well was filled with Brain Heart Infusion (BHI) broth and inoculated with bacterial suspension in a final volume of 2×10^6 cfu/mL. After adding compounds in triplicate, plates were subsequently incubated at 37 °C for 24 h under static conditions. The same amount of sterile BHI was added to top and bottom rows to avoid edge effects and to serve as negative controls. After the incubation period, the supernatant was removed and nonadherent cells were discarded by washing 3 times. The plates were dried and biofilms were stained with 0.1% crystal violet for 20 min and stained biofilms were solubilized with 33% acetic

acid. Absorbances were measured at 570 nm. The OD₅₇₀ values of *P. aeruginosa* PA01 alone were used as positive control.

4.5. Molecular Docking

The crystal structure of LasR with the co-crystallized ligand of N-3-(oxododecanoyl)-L-homoserine lactone (ODHL), was retrieved from Protein Data Bank under the PDB code 3IX3, with the resolution of 1.40 Å [27]. The chemical formulas of the molecules (**U10** and **U15**) decreasing PA01 biofilm formation were drawn using ChemDraw Ultra 12.0. These urea derivatives were docked into the active pocket of LasR using AutoDock Vina 1.1 [28], integrated into LigandScout 4.2 [29], with default parameters. The obtained poses were visually analyzed using LigandScout 4.2. The molecular docking figures in this study were generated by Maestro [30] and LigandScout 4.2.

4.6. *In silico* Prediction of Physicochemical Properties

The chemical formulas of the most active compounds were drawn in ChemDraw Ultra 12.0 and saved as Simplified Molecule Input Entry System (SMILES) file. Molinspiration (<https://www.molinspiration.com>) [31] was used for the calculation of molecular and drug-likeness properties of the compounds.

Declaration of Interest

The authors declared no potential conflicts of interest.

Acknowledgements

ŞDD is indebted to the Scientific and Technological Research Council of Turkey (Grant No: 115Z261) and the Faculty of Pharmacy at Erciyes University for their financial support of this work. The authors would like to acknowledge the contribution of the COST (European Cooperation in Science and Technology) Action CA 15106. MGG is grateful to Prof. Dr. Gerhard Wolber, Freie Universität Berlin, for providing the license for LigandScout 4.2.

References

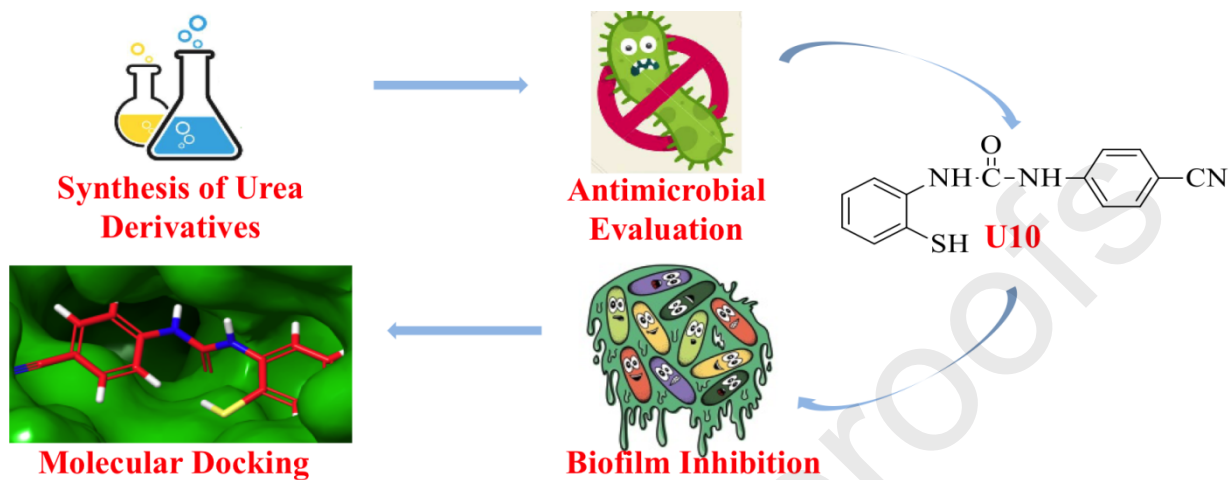
- [1] J.L. Martínez, F. Baquero, Interactions among Strategies Associated with Bacterial Infection: Pathogenicity, Epidemicity, and Antibiotic Resistance, *Clin. Microbiol. Rev.* 15 (2002) 647–679. doi:10.1128/CMR.15.4.647-679.2002.
- [2] N. Zhang, S. Ma, Recent development of membrane-active molecules as antibacterial agents, *Eur. J. Med. Chem.* 184 (2019) 111743. doi:10.1016/j.ejmech.2019.111743.
- [3] A.H. Limper, A. Adenis, T. Le, T.S. Harrison, Fungal infections in HIV/AIDS, *Lancet Infect. Dis.* 17 (2017) e334–e343. doi:10.1016/S1473-3099(17)30303-1.
- [4] WHO | Global tuberculosis report 2019, WHO. (2019).
https://www.who.int/tb/publications/global_report/en/.
- [5] D.W. MacPherson, B.D. Gushulak, W.B. Baine, S. Bala, P.O. Gubbins, P. Holtom, M. Segarra-Newnham, Population mobility, globalization, and antimicrobial drug resistance, *Emerg. Infect. Dis.* 15 (2009) 1727–1732. doi:10.3201/eid1511.090419.
- [6] V.S. Krishna, S. Zheng, E.M. Rekha, L.W. Guddat, D. Sriram, Discovery and evaluation of novel Mycobacterium tuberculosis ketol-acid reductoisomerase inhibitors as therapeutic drug leads, *J. Comput. Aided. Mol. Des.* 33 (2019) 357–366. doi:10.1007/s10822-019-00184-1.
- [7] M. Harmsen, L. Yang, S.J. Pamp, T. Tolker-Nielsen, An update on Pseudomonas aeruginosa biofilm formation, tolerance, and dispersal, *FEMS Immunol. Med. Microbiol.* 59 (2010) 253–268. doi:10.1111/j.1574-695X.2010.00690.x.
- [8] E. Kalaiarasan, K. Thirumalaswamy, B.N. Harish, V. Gnanasambandam, V.K. Sali, J. John, Inhibition of quorum sensing-controlled biofilm formation in Pseudomonas aeruginosa by quorum-sensing inhibitors, *Microb. Pathog.* 111 (2017) 99–107. doi:10.1016/j.micpath.2017.08.017.
- [9] L. Soulère, Y. Queneau, Conformational and docking studies of acyl homoserine lactones as a robust method to investigate bioactive conformations, *Comput. Biol. Chem.* 79 (2019) 48–54. doi:10.1016/j.compbiolchem.2019.01.006.
- [10] A.K. Ghosh, M. Brindisi, Urea Derivatives in Modern Drug Discovery and Medicinal Chemistry, *J. Med. Chem.* (2019). doi:10.1021/acs.jmedchem.9b01541.
- [11] E.J. North, M.S. Scherman, D.F. Bruhn, J.S. Scarborough, M.M. Maddox, V. Jones, A. Grzegorzewicz, L. Yang, T. Hess, C. Morisseau, M. Jackson, M.R. McNeil, R.E. Lee,

- Design, synthesis and anti-tuberculosis activity of 1-adamantyl-3- heteroaryl ureas with improved in vitro pharmacokinetic properties, *Bioorganic Med. Chem.* 21 (2013) 2587–2599. doi:10.1016/j.bmc.2013.02.028.
- [12] G.D. Francisco, Z. Li, J.D. Albright, N.H. Eudy, A.H. Katz, P.J. Petersen, P. Labthavikul, G. Singh, Y. Yang, B.A. Rasmussen, Y.-I. Lin, T.S. Mansour, Phenyl thiazolyl urea and carbamate derivatives as new inhibitors of bacterial cell-wall biosynthesis, *Bioorg. Med. Chem. Lett.* 14 (2004) 235–238. doi:10.1016/J.BMCL.2003.09.082.
- [13] H. Wang, Z.W. Zhai, Y.X. Shi, C.X. Tan, J.Q. Weng, L. Han, B.J. Li, X.H. Liu, Novel trifluoromethylpyrazole acyl urea derivatives: Synthesis, crystal structure, fungicidal activity and docking study, *J. Mol. Struct.* 1171 (2018) 631–638. doi:10.1016/j.molstruc.2018.06.050.
- [14] A. Ion, V. Parvulescu, P. Jacobs, D. De Vos, Synthesis of symmetrical or asymmetrical urea compounds from CO₂ via base catalysis, *Green Chem.* 9 (2007) 158–16. doi:10.1039/b612403h.
- [15] C.A. Lipinski, F. Lombardo, B.W. Dominy, P.J. Feeney, Experimental and computational approaches to estimate solubility and permeability in drug discovery and development settings, *Adv. Drug Deliv. Rev.* 46 (2001) 3–26. doi:10.1016/S0169-409X(00)00129-0.
- [16] D.F. Veber, S.R. Johnson, H.Y. Cheng, B.R. Smith, K.W. Ward, K.D. Kopple, Molecular properties that influence the oral bioavailability of drug candidates, *J. Med. Chem.* 45 (2002) 2615–2623. doi:10.1021/jm020017n.
- [17] D.F. Veber, S.R. Johnson, H.-Y. Cheng, B.R. Smith, K.W. Ward, K.D. Kopple, Molecular Properties That Influence the Oral Bioavailability of Drug Candidates, *J. Med. Chem.* 45 (2002) 2615–2623. doi:10.1021/jm020017n.
- [18] S.D. Doğan, E. Demirpolat, M.B. Yerer Aycan, M. Balci, Synthesis of new 4-aza-indoles via acyl azides, *Tetrahedron.* 71 (2015) 252–258. doi:10.1016/J.TET.2014.11.057.
- [19] D.E. Ames, W.D. Dodds, Condensation of β -dicarbonyl compounds with halogenopyridinecarboxylic acids. A convenient synthesis of some naphthyridine derivatives, *J. Chem. Soc. Perkin Trans. 1.* (1972) 705–710. doi:10.1039/P19720000705.
- [20] L.W. Deady, T. Rodemann, The reaction of homophthalic acid and some aza analogues with vilsmeier reagent: A reinvestigation, *J. Heterocycl. Chem.* 38 (2001) 1185–1190. doi:10.1002/jhet.5570380524.

- [21] Ş.D. Doğan, Copper-catalyzed NH/SH functionalization: A strategy for the synthesis of benzothiadiazine derivatives, *Tetrahedron*. 73 (2017) 2217–2224.
doi:10.1016/J.TET.2017.02.063.
- [22] Ş.D. Doğan, Y. Çetinkaya, S. Buran, S.Ö. Yıldırım, R.J. Butcher, Chemoselective synthesis, X-ray characterization and DFT studies of new organic single crystal: S-(2-aminophenyl) cyclohexylcarbamoithioate, *J. Mol. Struct.* 1204 (2020) 127499.
doi:10.1016/j.molstruc.2019.127499.
- [23] Clinical and Laboratory Standards Institute, Methods for dilution antimicrobial susceptibility tests for bacteria that grow aerobically, Approved Standard 8th ed., M 07-A8. Clinical and Laboratory Standards Institute, Wayne, PA, 2008.
- [24] Clinical and Laboratory Standards Institute, Reference method for broth dilution antifungal susceptibility testing of yeasts: approved Standard 3rd ed., M 27-A3. Clinical and Laboratory Standards Institute, Wayne, PA, 2008.
- [25] L. Collins, S.G. Franzblau, Microplate alamar blue assay versus BACTEC 460 system for high-throughput screening of compounds against *Mycobacterium tuberculosis* and *Mycobacterium avium*., *Antimicrob. Agents Chemother.* 41 (1997) 1004–1009.
doi:10.1128/AAC.41.5.1004.
- [26] C. Rigon Mizdal, S. Terra Stefanello, P. Cordenonsi Bonez, V. Albertina Agertt, V. da Costa Flores, G. Guidolin Rossi, F. dos Santos Siqueira, L. de Lourenco Marques, M. Matiko Anraku de Campos, Anti-biofilm and Antibacterial Effects of Novel Metal-coordinated Sulfamethoxazole Against *Escherichia coli*, (n.d.).
- [27] <https://www.rcsb.org/structure/3ix3>.
- [28] O. Trott, A.J. Olson, AutoDock Vina: Improving the speed and accuracy of docking with a new scoring function, efficient optimization, and multithreading, *J. Comput. Chem.* 31 (2009) 455–461. doi:10.1002/jcc.21334.
- [29] G. Wolber, T. Langer, LigandScout: 3-D pharmacophores derived from protein-bound ligands and their use as virtual screening filters., *J. Chem. Inf. Model.* 45 (2005) 160–9.
doi:10.1021/ci049885e.
- [30] Schrödinger Release 2018-3: Maestro, Schrödinger, LLC, New York, NY, 2018., (2018).
- [31] Molinspiration, <https://www.molinspiration.com/cgi-bin/properties>.

Journal Pre-proofs

Graphical abstract



Highlights

- Synthesis of 1,3-disubstituted urea derivatives
- Evaluation of antibacterial, antifungal and antitubercular activities
- Determination of biofilm inhibition on *P. aeruginosa* PAO1
- Molecular docking supported quorum sensing inhibition
- *In silico* calculation of molecular properties